Probabilistic performance assessment of low ductility r.c. frames retrofitted by elasto-plastic dissipative braces

Laura Ragni, Fabio Freddi, Enrico Tubaldi
Dipartimento di Architettura, Costruzione e Strutture, Università Politecnica delle Marche. Via Brecce Bianche, 60131 Ancona.

Andrea Dall'Asta
Scuola di Architettura e Design, Università di Camerino. Viale della Rimembranza, 63100 Ascoli Piceno

Keywords: Vulnerability of low ductility r.c. frames, seismic retrofit, fragility curves, elasto-plastic devices.

ABSTRACT
The paper illustrates a probabilistic methodology for assessing the vulnerability of existing r.c. buildings with limited ductility capacity and retrofitted by means of dissipative braces. The methodology is based on the development of single component and system fragility curves before and after the retrofit. The proposed approach allows to highlight the possible changes in the most significant collapse modalities before and after the retrofit and to evaluate the effectiveness of the retrofit by taking into account the probabilistic properties of the seismic behaviour of the considered systems.
A benchmark 2-dimensional reinforced concrete frame with low ductility capacity is considered as case study. The frame is designed for gravity-loads only and does not comply with modern anti-seismic code requirements. It is retrofitted by introducing elasto-plastic dissipative braces designed for different levels of their target base-shear capacity, following a design method involving the pushover analysis of the system before and after retrofit. The obtained results show that the use of braces yields a significant increase in the seismic capacity, though an increased dispersion of the behaviour is observed in the retrofitted system.

1 INTRODUCTION

The damage occurred during recent earthquakes in many existing reinforced concrete (r.c.) buildings designed before the introduction of modern anti-seismic codes has shown that these structures are very vulnerable to the seismic action due to their reduced ductility capacity. Thus, there is a significant need of modern retrofit techniques for reducing the vulnerability of these structure and of reliable tools for assessing the effectiveness of the retrofit.

Passive control systems have proven to be a very efficient tool for the seismic retrofit of existing r.c. frames. Among the various types of dissipative devices currently applied in the retrofit of existing structures (Soong and Spencer 2002, Christopoulos and Filiatrault 2006), those with elasto-plastic behaviour appear to be very promising due to the large hysteresis cycles they can undergo during the earthquake action. Elasto-plastic dissipation devices provide a supplemental path for the earthquake induced horizontal actions and thus enhance the seismic behaviour of the frame by adding stiffness and dissipation capacity to the bare frame. It should be noted that the introduction of an elasto-plastic bracing system into a low ductility frame may induce remarkable changes both in the collapse modalities and in the probabilistic properties of the seismic behaviour of the structure. The latter aspect assumes a considerable importance in consequence of the high degree of uncertainty affecting the seismic input and of the differences in the propagation of this uncertainty through the two resisting systems (r.c. frame and elasto-plastic dissipative bracing).

For these reasons, the evaluation of the effectiveness of this type of retrofit technique in reducing the frame vulnerability should be performed within a probabilistic framework and should be capable of addressing the specific issues deriving from the use of dissipative braces. Usually, the probabilistic assessment of the

seismic vulnerability of structural systems involves the development of fragility curves. These probabilistic tools provide the probability that a specified limit state or failure condition is exceeded, conditional to the strong-motion shaking severity, measured by means of an appropriately selected intensity measure (*IM*). Some recent studies have been developed which employ fragility curves in evaluating the effects of various techniques for retrofitting existing frames. In particular, Hueste and Bai 2007 investigated the effectiveness of different retrofit techniques in reducing the seismic fragility of a typical 1980s r.c. building in Central US. Ramamoorthy et al. 2006 assessed the seismic vulnerability of a two-story reinforced concrete frame building designed for gravity loads only. They also developed fragility curves for the same building retrofitted by means of column strengthening, showing the effectiveness of this technique in reducing the frame vulnerability. Guneyisi and Altay 2008 developed fragility curves for evaluating the effectiveness of several retrofitting measures based on the use of viscous dampers in reducing the vulnerability of a realistic high-rise reinforced concrete building.

The probabilistic methodology proposed in this paper represent a novel application of these probabilistic tools to the specific problem analyzed: fragility curves of the system before and after the retrofit are employed to evaluate the impact of the introduction of the elasto-plastic braces. For this purpose, fragility carves are developed by monitoring the seismic demand through local engineering demand parameters (EDPs) (Mackie and Stojadinovic 2003) such as the maximum strain demand at the most critical sections. Local EDPs have been preferred to global EDPs (such as the inter-storey drift) usually employed, since these latter would not be able to capture the modifications to the frame response and capacity induced by the introduction of the bracing system. Furthermore, in addition to system fragility curves, component fragility curves are developed for single structural members (e.g., beam, column, brace or group of these elements) in order to monitor the most vulnerable elements before ad after the retrofit and, thus, to highlight the possible changes in the most probable collapse modalities. Finally, some synthetic parameters describing the fragility curves are defined in order to compare the performance of the bare and of the retrofitted frames by taking into account the probabilistic properties of the seismic behaviour of the bare and retrofitted structure.

The capability and effectiveness of the proposed methodology is tested by considering a benchmark r.c. frame with limited ductility capacity (Bracci et al. 1992). This benchmark frame has been already used as case study by other authors, since extended experimental results are available for the calibration of a reliable numerical model. The r.c. frame is retrofitted by inserting a bracing system designed for several levels of the base shear capacity. The braces are designed by applying a method often employed and based on the nonlinear static analysis of the system before and after retrofit (Braga and D'Anzi 1994, Kasai et al. 1998, Mazza and Vulcano 2008, Dall'Asta et al. 2009, Ponzo et al. 2010).The proposed methodology also allow to test the effectiveness of this simplified criterion employed for the design of braces.

2 RETROFITTING OF R.C. FRAME WITH ELASTO-PLASTIC BRACES

The design procedure, synthetically illustrated below, can be applied to the design of dissipative braces exhibiting an elasto-plastic behaviour. The interested reader is referred to Dall'Asta et al. 2009 for a more detailed description. The dissipative braces considered in this paper are made by an elasto-plastic dissipation device placed in series with an elastic brace exhibiting adequate overstrength. The properties of the dissipative brace can be defined based on the properties of its components. In particular, if K_b denotes the axial stiffness of the elastic brace and K_0, F_0 and μ_{0u} respectively the stiffness, yielding force and ductility capacity of the elasto-plastic device, the dissipative brace stiffness K_d and ductility capacity μ_{du} are given by:

$$K_d = \frac{K_b K_0}{K_b + K_0} \quad \text{and} \quad \mu_{du} = \frac{K_0 + K_b \mu_{0u}}{K_b + K_0} \tag{1}$$

while the yielding force F_d is equal to F_0. Usually, the value of μ_{0u} is in the range 15-20 while the value of μ_{du} is in the range 10-15, depending on the ratio K_0/K_b. The method followed for designing the dissipative system is based on pushover analysis of the existing frame under a distribution of forces corresponding to its first vibration mode, in order to assess its capacity. The "collapse point" for the frame is defined by the values of the maximum displacement at the top floor d_u and by the maximum base shear V^1_f the frame is capable to withstand. The dissipative bracing system is assumed to behave as an elastic-perfectly plastic system, with shear capacity equal to V^1_d, ductility capacity equal to μ_{du} and with the same collapse

displacement of the bare frame (d_u). This last assumption aims at obtaining a simultaneous failure of both the frame and the dissipative braces. It is noteworthy that the value of V^1_d is a design choice and depends on the objective of the retrofit. For a given value of V^1_d, the stiffness of the bracing system at the first storey is given by:

$$K_d^1 = \frac{V_d^1 \mu_{du}}{d_u \delta^1} \tag{2}$$

where δ^1 is the inter-storey drift at the first storey, normalized with respect to the top floor displacement according to the first modal shape. The shear V^i_d and stiffness K^i_d of the dissipating bracing system at each storey can be determined by the following relations:

$$V_d^i = V_d^1 v^i \quad \text{and} \quad K_d^i = K_d^1 k^i \tag{3}$$

where v^i and k^i are the shear force and stiffness at each storey, normalized with respect to the base shear and base stiffness according to the first mode of the bare frame. By this way, the stiffness distribution of the dissipative braces at each storey ensures that the first modal shape of the bare frame remains unvaried after the retrofit. This avoids drastic changes to the internal action distribution in the frame, at least in the range of the elastic behaviour. Additionally, the chosen strength distribution of the dissipative braces aims at obtaining simultaneous yielding of the devices at all the storeys and, thus, a global ductility of the bracing system coinciding with the ductility of the single braces. Given V^i_d and K^i_d, the braces properties (K^i_0, F^i_0 and K^i_b) at each storey can be determined based on the number of braces and on geometrical considerations.

3 PROBABILISTIC METHODOLOGY FOR VULNERABILITY ASSESSMENT

The evaluation of the performance of the frame before and after the retrofit requires a probabilistic approach due to the high degree of uncertainty characterizing the earthquake input and the system properties. The earthquake input motion is usually characterized by a degree of uncertainty that overcomes the aleatoric uncertainty in material and geometrical system properties. Thus, only the former source of uncertainty is considered in this study by selecting a set of natural ground motion (g.m.) records which reflect the variability in duration, frequency content, and other characteristic of the earthquake input which is likely to act on the system. The selected records are compatible with an input uniform hazard spectrum, thus they are characterized by a given intensity and can be assigned an annual frequency of occurrence depending on the site. In order to evaluate the system performance for other seismic intensity values and, thus, to generate fragility curves, incremental dynamic analysis (IDA) (Vamvatsikos and Cornell 2001) is performed by subjecting the system to the selected g.m. records for increasing values of the seismic intensity. In this study, the spectral acceleration at the fundamental period of the structure $S_a(T)$ is used as seismic intensity measure *IM* (Katsanos et al. 2009). This choice requires the normalization of the g.m. records in order to obtain the same value of $S_a(T)$ for the natural period of the structure T, which is different for the bare and the retrofitted frames. The results of IDAs are multi-record IDA curves, i.e., the plot of appropriately selected engineering demand parameters (EDPs) monitoring the system response vs *IM*. Usually, a global EDP such as the maximum inter-story drift is employed to assess the vulnerability of structural systems by means of fragility curves (Kwon and Elnashai 2006, Hueste and Bai 2007). However, in this paper the inter-storey drift is not considered as EDP since it would not be able to capture the modifications to the frame response and capacity induced by the introduction of the bracing system, (e.g., the axial load at the columns connected to the braces). For this reason local EDPs are chosen in the present study. In particular, the local EDPs selected are *a)* the maximum-over-time values of the axial concrete strain ε_c and steel strain ε_s, at each element, *b)* the maximum-over-time values of each element's shear force *c*) the maximum-over-time value of tension (σ_t) and compression (σ_c) stresses at each beam-column joints and *d)* the ductility demand at each dissipative brace μ_d.

Based on IDA results, component and system fragility curves are developed for the bare and for the retrofitted frame. In particular, the component fragility curves are obtained by comparing the samples of EDPs deriving from IDA with the corresponding capacity. The limit states considered are: *LS1)* ε_c exceeding the limit ε_{cu} at any element, *LS2)* ε_s exceeding the limit ε_{su} at any element, *LS3)* the shear demand at any element exceeding the shear resistance *LS4)* σ_t and σ_c exceeding the tension (f_{ctu}) and compression (f_{cu}) resistance of joints and *LS5)* the ductility demand of the dissipative braces μ_d overcoming the ductility capacity μ_{du} at any storey. The system curves are developed by assuming a series arrangement of the components, i.e. failure in one component yields system failure. In order to synthetically describe the system fragility curves,

two parameters are defined: the median *IM* at collapse ($IM_{c,50}$), i.e. the *IM* corresponding to 50% probability of failure, and the dispersion measure (β_c) given by:

$$\beta_c = \frac{1}{2}\ln\left(\frac{IM_{c,84}}{IM_{c,16}}\right) \quad (4)$$

where $IM_{c,84}$ and $IM_{c,16}$ are the *IM* values corresponding to the 84th and the 16th fractiles of the fragility curve, i.e., the values of the *IM* which yield failure respectively in 84 and 16 cases over 100. These two parameters are used to compare the performance of the bare and of the retrofitted frame and, thus, to assess in probabilistic terms the effectiveness of the retrofit. In particular, the first parameter, $IM_{c,50}$, divided by the value $S_a(T)$ of a reference spectrum at the system natural period *T*, provides the so called "collapse margin ratio" m_{50} (Liel et al. 2010, Ciampoli et al 2003), i.e., the factor the reference spectrum has to be scaled by in order to induce system collapse in 50% of the cases. This normalized measure allows to account for the change in the seismic input (spectral) intensity due to the variation in the natural period of the system, and thus permits to compare systems with different structural periods. In this study, the reference spectrum is assumed as the uniform hazard spectrum scaled such that m_{50}=1, i.e. $IM_{c,50}$= $S_a(T)$, for the bare frame. By assuming this reference spectrum and by assuming that its spectral shape does not change with the seismic input intensity, the normalized parameter m_{50} also provides for the retrofitted frames the ratio between the peak ground acceleration (PGA) yielding collapse in 50% of the cases in the retrofitted frames and the PGA yielding collapse in 50% of the cases in the bare frame. In a similar way, based on the ratio $IM_{c,16}$/ $S_a(T)$ and $IM_{c,84}$/ $S_a(T)$, the factors m_{16} and m_{84} corresponding to the 16th and 84th fractiles are defined. Finally, the parameter i_{50} describing the increment of the PGA yielding collapse in 50% of the cases, due to the retrofit, is defined as i_{50} = m_{50} –*1*. In a similar way, the parameters i_{16} and i_{84} are defined. These factors permit to estimate the effectiveness of the retrofit in reducing the frame seismic vulnerability with higher and lower confidence with respect to i_{50}.

4 APPLICATION TO A CASE STUDY

4.1 Case study description

A three storey ordinary r.c. moment resisting frame has been considered as case study (Bracci et al. 1992a). The building has been designed for gravity loads only and without any seismic detailing, applying the design rules before the introduction of modern anti-seismic codes. The dimension adopted for the frame members of the prototype structure are based on a survey of typical construction practices in the eastern United States conducted by El-Attar et al.1990 and 1991 so that the structure is presented from the author as representative of low-rise buildings constructed in the Eastern and Central United States. The considered frame of the building consists of three stories 3.66 m high for a total height of 11 m and three bays, each 5.49 m wide. Columns have a 300×300 mm^2 square section while beams are 230×460 mm^2 at each floor. The provision of ACI 318-89 code, Grade 40 steel (f_y = 276 MPa) and concrete with compression resistance f_c‘ = 24 MPa, were employed in the design. Since earthquake loads are neglected and the wind loads on a three storey structure are relatively small, no lateral load are considered for the design. Figure 1 a) contains the general layout of the structure and Figure 1 b) shows some beam reinforcement detailing

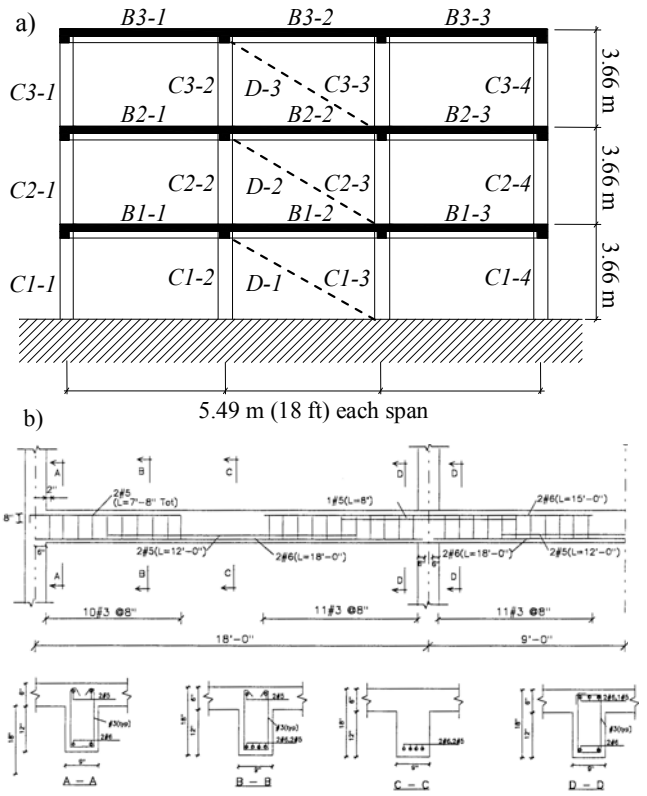

Figure 1 a) General layout of the structure and braces arrangement, b) beam reinforcement detailing.

Extended experimental results of this two dimensional frame under earthquake loading are available. In particular, experimental information include a 1:3 reduced scale model tested on shaking table by Bracci et al. 1992a, 1992b and the evaluation of the performance of several

subassemblages, i.e. column and beam-column joints subassemblage tested from Aycardi et al. 1992. The structure has already been used as case study by other authors (Kwon and Elnashai, 2006, Alam et al., 2009).

4.2 Finite element model

For this study a two dimensional model of the structure is employed. The structural finite element model of the frame, built within OpenSees (McKenna et al., 2006), employs hinges elements (Scott and Fenves, 2006) to model the hysteretic behaviour of beams and columns. The fiber section of the element employs Concrete02 and Hysteretic as models for materials. The plastic hinge length for both beam and column has been evaluated based on the formula proposed in Panagiotakos and Fardis, 2001 :

$$L_p = 0.12L_V + 0.014\alpha d_{bl} f_y \qquad (5)$$

where L_V is the element shear length, α is a parameter which assumes the value 0 (or 1) in presence (absence) of lap-spliced rebars at the element's end sections, d_{bL} is the longitudinal bar diameter and f_y is the steel yield strength. The elastic part of each element is assigned an effective flexural stiffness value, evaluated through moment-curvature analysis, for the axial force level induced by the dead loads. The rigid-floor diaphragm is modelled by assigning a high value to the axial stiffness of the beams and the masses are deposited at the beam-column connections.

In order to validate the accuracy of the finite element model in terms of the local and global behaviour, 1:3 scaled models of subassemblages and a 1:3 scaled model of the two dimensional frame are developed using the same software package and the same rules adopted for the full scale model. Numerical results of the reduced scaled models are compared with the experimentally obtained results following the laboratory tests conducted by Aycardi et al. 1992 and Bracci et al. 1992a, 1992b. In particular, in Aycardi et al. 1992 four 1:3 scale column specimens with and without lap splices and loaded with low and high levels of axial forces, representing interior and exterior column at floor slab and beam soffit levels, were examined under reversed cyclic loading at increasing drift amplitudes until failure. In addition, two specimens at 1:3 scale that model typical exterior and interior beam-column subassemblages, were subjected to axial load and reversed cyclic lateral displacements. In the 1:3 scaled numerical models developed for simulating these experimental tests, concrete characteristics are selected according to the values experimentally obtained for each element. Figure 2, Figure 3 and Figure 4 show the comparisons between experimental and analytical results respectively for column specimen 1, interior and exterior subassemblages, in term of the lateral force *vs* the lateral drift (i.e. the ratio between the lateral displacement and the inter-storey height).

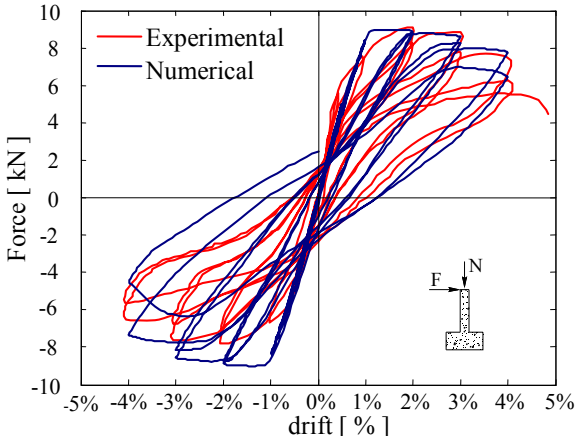

Figure 2. Experimental and numerical lateral load-drift comparison for column specimen 1.

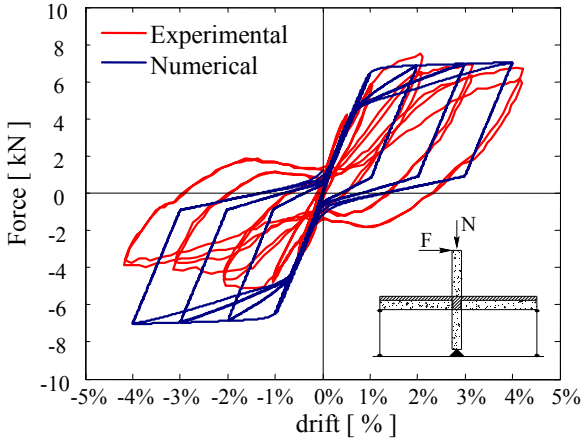

Figure 3. Experimental and numerical lateral load-drift comparison for interior slab-beam-column subassemblage.

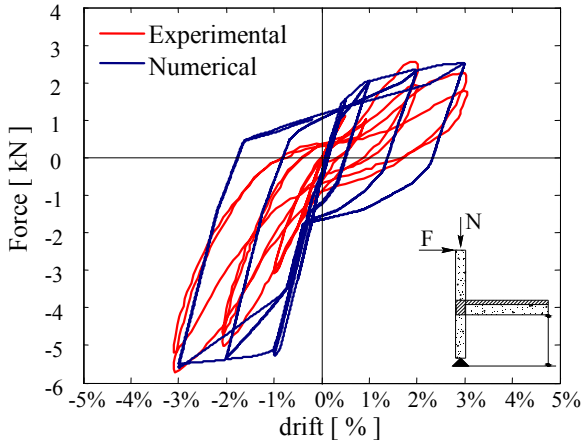

Figure 4. Experimental and numerical lateral load-drift comparison for exterior slab-beam-column subassemblage.

Good agreement with the experimental results verifies that the analytical model well represents

the local behaviour of the structure. In Bracci et al. 1992a and 1992b results of experimental tests carried out in order to investigate the global behaviour of 1:3 scaled model of the prototype are reported. In particular, snap back and white noise tests on the 1:3 scaled model were conducted to obtain the natural periods and the respectively modal shapes. The first three natural periods obtained are 0.538, 0.177 and 0.119 sec. Shaking table tests were also performed by applying the Kern County 1952, Taft Lincoln School Station, N021E component record scaled for PGA of 0.05g, 0.20g and 0.30g. In the 1:3 scaled model developed in this study, average values of the concrete characteristics experimentally obtained for different frame elements are used. The elastic structural periods from eigenvalue analysis of the numerical model are 0.561, 0.180, and 0.110 sec for the first, second, and third modes, respectively. These periods are very close to the values provided by the experimental tests and give credence to the numerical model. Additionally, Figures 5 a) and b) show the comparison between the 3rd story displacements of the 1:3 scale experimental and numerical model corresponding to ground motions with PGA of 0.05g and 0.20g, respectively. For small amplitude ground excitation the Rayleigh damping is taken from the snap-back test, while for the higher ground motion excitation Rayleigh damping of 3% is used. Additionally, for the modal parameters evaluation and for the time history analyses with low values of PGA, gross stiffness of elements are employed in the numerical model. Conversely, effective stiffness are used in the numerical model for time history analyses with higher values of PGA. Also in this case a good agreement between experimental and numerical results are obtained. Finally, the full scale model is validate by comparing structural periods and time histories of floor displacement with the experimental results after conversion to full scale using similitude laws.

4.3 Retrofit

In Figure 6 the pushover curve obtained for the load distribution relative to the first vibration mode of the bare frame (mass participation factor of 86.4%) is shown and the limit corresponding to the failure of the columns C1-2 and C1-3 of Figure 1, which occurs first, is posed in evidence. This limit, which is attained for an inter-storey drift of about 1.0%, is due to concrete failure ($\varepsilon_c=\varepsilon_{cu}$) and corresponds to a displacement δ_u of 0.102 m and a shear capacity V_f^1 of 186 kN. The failure of the beam-column joints as well the shear failure of the frame elements are not controlled in the push over analysis, local retrofit measures will be eventually provided. It is observed that the frame ductility capacity corresponding to the chosen strain capacity is very limited. The bare frame is retrofitted by inserting a bracing system designed for several values of the ratio v between the shear capacity of the bracing system V_d^1 and that of the frame V_f^1, measuring the increment of base shear due to the retrofit (form 0.2 to 1.4).

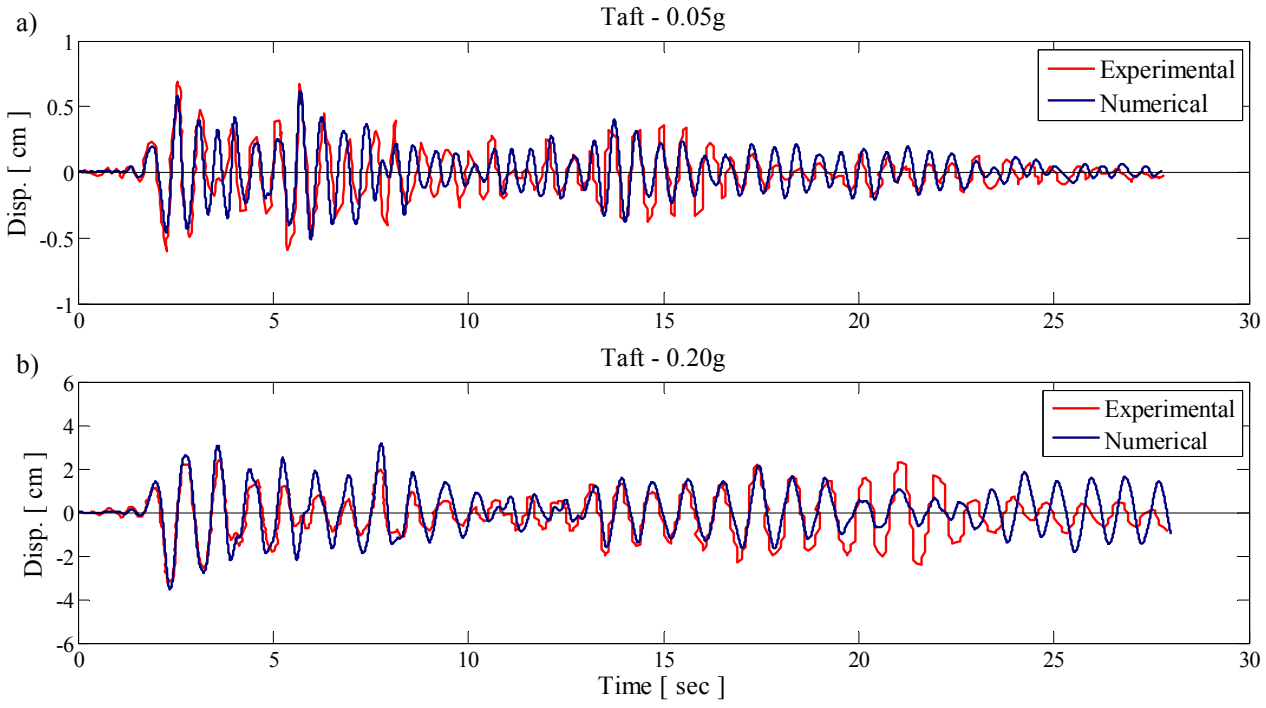

Figure 5. Comparison of dynamic analysis: a) 3rd storey displacement – 0.05g, b) 3rd storey displacement – 0.20g

The ductility capacity assumed for the dissipative bracing system is μ_{du} = 12. The dissipative devices considered in this study are Buckling-Restrained Axial Dampers (BRADs) (Antonucci et al. 2007) made of an internal steel core whose buckling is prevented by an external steel casing filled with mortar. These devices are usually short, so that they are able to yield for small displacements and thus can be used in the retrofit of r.c. frames with limited ductility collapsing for small lateral displacements. The maximum ductility capacity of this kind of devices is about μ_{0u} = 15. The pushover curves of the retrofitted frame for the different levels of v are shown in Figure 6. The braces properties of three retrofit levels (v = 0.4,0.8 and 1.2) are shown in Table 1.

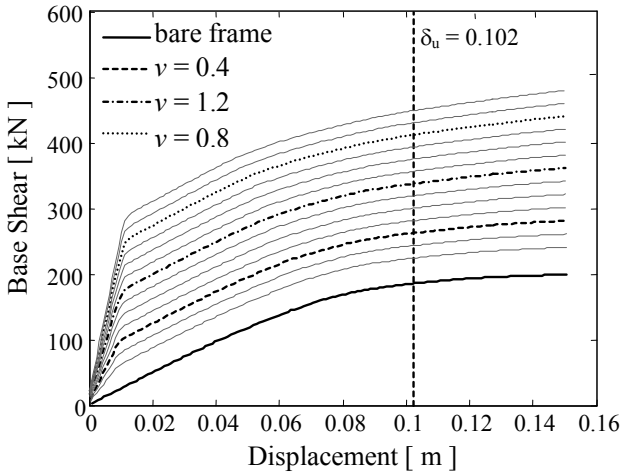

Figure 6. Pushover curves for bare and retrofitted frame.

Table 1. Brace properties at each storey

	v=0.4		v=0.8		v=1.2	
Storey	F_d^i	K_d^i	F_d^i	K_d^i	F_d^i	K_d^i
	[kN]	[kN/m]	[kN]	[kN/m]	[kN]	[kN/m]
1	88	36046	175	72091	263	108137
2	75	25106	150	50212	226	75317
3	43	22921	86	45843	130	68764

4.4 Fragility curves

For the purpose of developing fragility curves, a number of 30 natural g.m. records are selected from the European database (Ambraseys et al. 2000). These records are compatible with the Eurocode 8 - type 1 (ECS 2005) soil type D (S =1.35) response spectrum with a peak ground acceleration PGA=0.1Sg. They have been chosen in a range of magnitude and source to site distance of 5.5-7.0 and 25-75km respectively. The spectral acceleration at the fundamental period of the structure $S_a(T)$ is used as seismic intensity measure IM. Thus, the records are scaled so that they have the same IM, i.e. the same spectral acceleration at the fundamental period of the system. It is noteworthy that the vibration period and consequently the IM are different for the bare and the retrofitted frames. Moreover for the retrofitted frame they vary with v (for cases reported in Table 1, the natural periods are T_1=0.670s, T_1=0.521s and T_1=0.448s). Thus, for each case, g.m. records are scalded according to the IM of the considered case. Figure 7 shows the code input spectrum, the spectra of the scaled records and the corresponding mean spectrum, for the case of the bare frame.

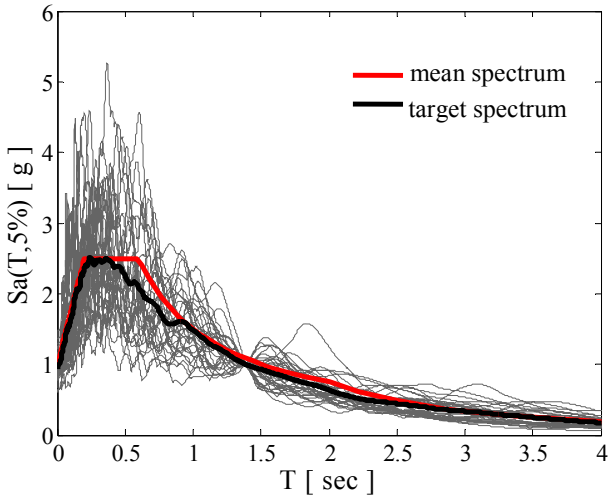

Figure 7. Normalized spectra for the bare frame.

In developing the fragility curves, the limits of the concrete and steel capacity are set equal to ε_{cu} = 0.0035 and ε_{su} = 0.04 (ECS 2005).The shear resistance of beams and columns and the resistance in tension and in compression of beam-column-joints are evaluated according to the formulas proposed by Priestley et al. (1996). The numerical fragility curves can be approximated with good accuracy by fitting a lognormal fragility curve. For example, Figure 8 shows the numerical system fragility curve and the fitted lognormal fragility curve for the case of the bare frame.

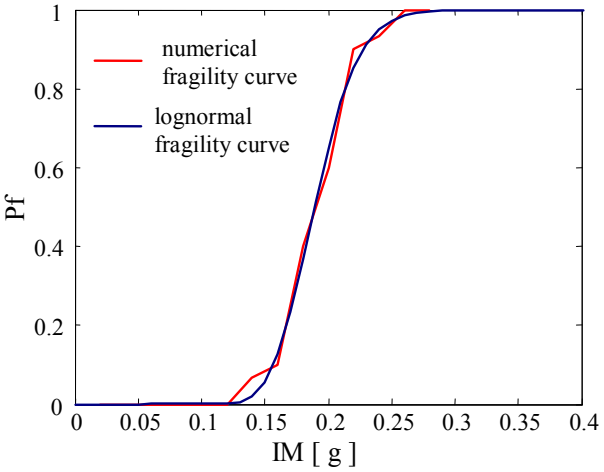

Figure 8. Lognormal fitting of numerical fragility curve.

Hereafter, the results will be shown only in terms of lognormal fragility curves.

In Figure 9, the fragility curves of the bare frame in terms of concrete failure, steel failure and joint failure are reported. The most significant failure mode corresponds to the joints failure in tension while joints failure in compression and shear failure have a zero probability of occurrence. It is noted that in this study joint cracking is not considered as a collapse limit state. Consequently, concrete failure (*LS1*) becomes the most likely to occur collapse modality, while steel failure (*LS2*) is much less probable.

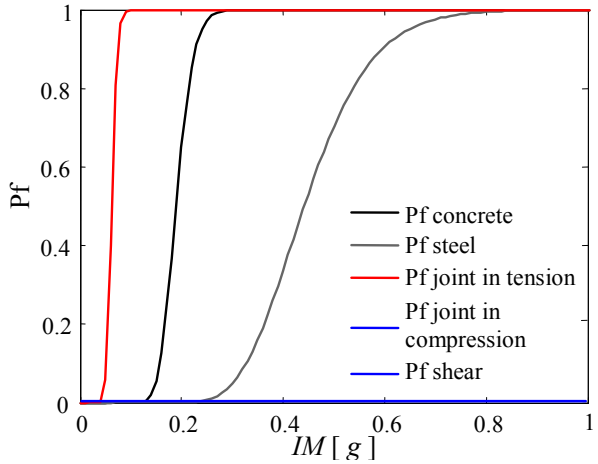

Figure 9. Components fragility curves – Failure modalities.

Figure 10 shows the fragility curve of the system and of the most vulnerable components, i.e., column *C1-2* and column *C1-3*. The prevailing failure mode for these components is concrete rupture and its contribution to the system fragility is very significant.

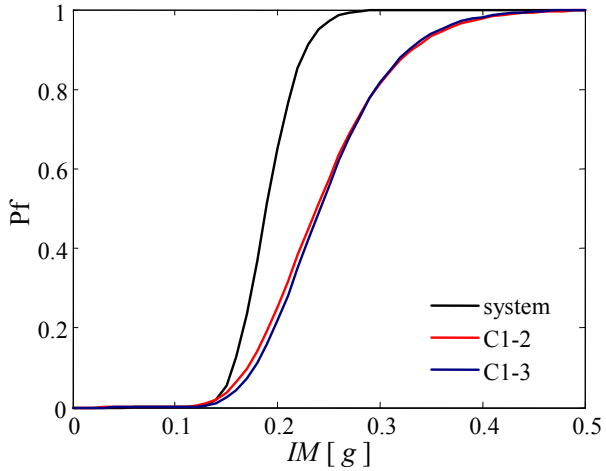

Figure 10. Fragility curve of the system and of the most vulnerable components.

Figure 11 shows the fragility curve of the system and of the most vulnerable elements, for the retrofitted frames corresponding to v=0.4, v=0.8 and v=1.2.

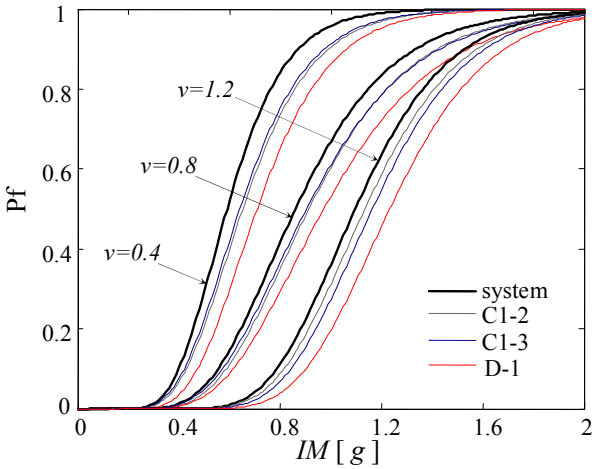

Figure 11. Fragility curve of the system and of the most vulnerable components for different retrofit levels.

It is observed that the rupture of concrete in column *C1-2* and column *C1-3* remains the most significant failure mode for all the levels of retrofit. Furthermore, in all the cases, the fragility curve of the most vulnerable dissipative brace (i.e., *D1*) is always close to the fragility curve of the most vulnerable elements of the frame. This finding means that frame components and dissipative devices have a comparable vulnerability and confirms the effectiveness of the simplified design method, where a simultaneous failure of both the frame and the braces is assumed. Figure 12 reports the system fragility curves of the bare frame and of the retrofitted frames, for the different v values.

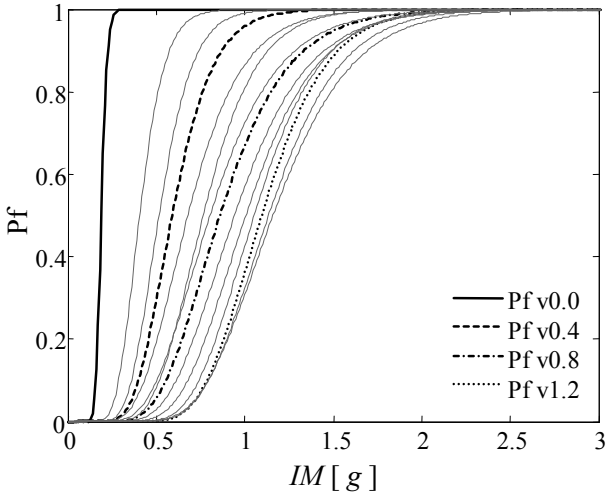

Figure 12. System fragility curves for the bare frame and for the retrofitted frames.

Globally, an increase in the value of $IM_{c,50}$ is observed for the increasing values of v, as expected. To better compare the obtained fragility curves, the parameters i_{16}, i_{50}, i_{84} and β_c, defined according to section 3, are evaluated. Figure 13 shows the variation with v of parameters i_{16}, i_{50} and i_{84}, providing the increment, due to the

retrofit, of the PGA leading to collapse respectively in 16%, 50% and 84% of cases.

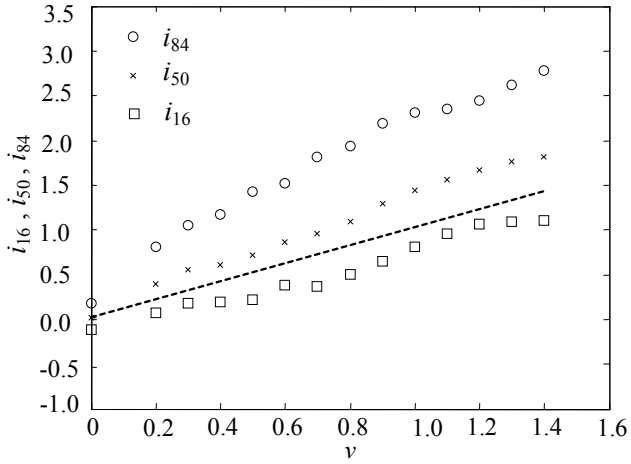

Figure 13. Variation of the seismic increment capacity.

These parameters exhibit a high correlation with v and they increase linearly for increasing values of v. In particular, it is observed that the values of i_{50} are close to dotted line corresponding to the same increase in the parameters v and i. This result is of interest in the design of the retrofit system, since it provides an immediate way to assess the increment of PGA for different retrofit levels and for different target confidence levels. Finally, Figure 14 plots the dispersion measure β_c evaluated according to Equation (4) vs. parameter v and shows that a significant increase of the dispersion occurs when elasto-plastic braces are introduced into the bare frame. In fact, the value of β_c for all the cases of retrofit is significantly larger than the corresponding value of the bare frame.

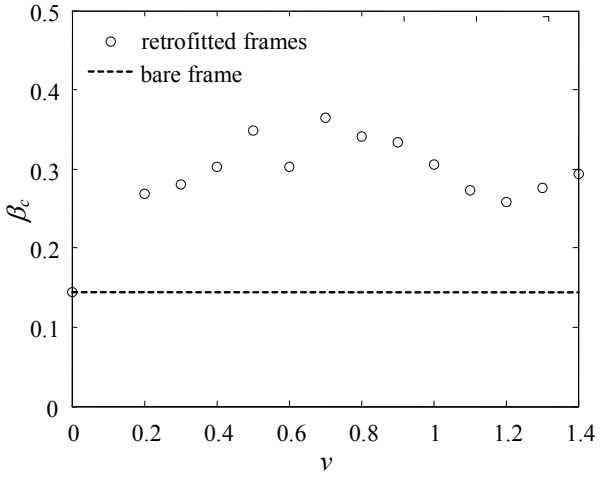

Figure 14. Variation of dispersion at collapse (β_c).

This can be explained recalling that the dissipative braces yield a more pronounced nonlinear behaviour and this may add dispersion to the response. Furthermore, accounting for the vulnerability of the braces in addition to that of the frame components necessarily results in an increase of global dispersion of capacity.

5 CONCLUSIONS

The paper illustrates a probabilistic methodology for assessing the vulnerability of existing r.c. buildings with limited ductility capacity and retrofitted by means of dissipative braces. The methodology is based on the development of fragility curves of the bare and the retrofitted frame. It employs non linear incremental dynamic analysis under a set of input ground motions to account for the randomness of the earthquake excitation and local EDPs to capture the modifications of the frame response induced by the introduction of the bracing system. Furthermore, in addition to global system fragility curves, component fragility curves are built for single structural components, in order to monitor the most vulnerable elements before ad after the retrofit. The methodology developed in this paper allows to evaluate the safety level reached by the frame before and after the retrofit by taking into account the probabilistic properties of the seismic response. At the same time, it can be used to evaluate the effectiveness of the criterion employed to design the dissipative braces.

The proposed methodology is applied in this paper to a benchmark r.c. frame with limited ductility capacity and retrofitted by elasto-plastic braces for different values of the shear capacity of the bracing system. The obtained results show that the seismic capacity significantly increases for increasing values of the base shear carried by the bracing system. However, a significant increment of the dispersion of the seismic response is observed when elasto-plastic braces are introduced, due to the more pronounced nonlinear behaviour induced by the dissipative bracing system and the additional limit state introduced in the vulnerability assessment accounting for failure of the braces. This change in the dispersion may significantly affect the estimate of the seismic risk of the system, which will be object of further investigation. Finally, the comparable vulnerabilities of the frame and of the dissipative braces obtained for the various retrofit levels confirm the effectiveness of the simplified criterion often employed to design this type of braces.

REFERENCES

ACI Committee 318, 1989, Building Code Requirements for Reinforced Concrete and Commentary (ACI 318-89/ACI 318R-89), *American Concrete Institute, Detroit*, 353.

Alam, M. S., M. Nehdi, et al., 2009. Seismic performance of concrete frame structures reinforced with superelastic shape memory alloys. *Smart Structures and Systems* **5**(5): 565-585.

Ambraseys, N., Smith, P., Berardi, R., Rinaldis, D., Cotton, F. and Berge-Thierry, C., 2000. Dissemination of European Strong-Motion Data. *CD-ROM Collection. European Council, Environment and Climate Research Programme.*

Antonucci, R., Cappanera, F., Balducci, F., Castellano, M.G., 2007. Adeguamento sismico del Liceo classico "Perticari" di Senigallia (AN). *XII Convegno Nazionale ANIDIS: L'Ingegneria sismica in Italia*, Pisa, Italy.

Aycardi, L.E., Mander, J.B., Reinhorn, A.M., 1992.Seismic resistance of reinforced concrete frame structures designed only for gravity loads: part II -Experimental Performance of Subaassemblages. Technical report NCEER-92-0028.

Bracci, J.M., Reinhorn, A.M., Mander, J.B., 1992a. Seismic resistance of reinforced concrete frame structures designed only for gravity loads: part I-design and properties of a one-third scale model structure. Technical report NCEER-92-0027.

Bracci, J.M., Reinhorn, A.M., Mander, J.B., 1992b. Seismic resistance of reinforced concrete frame structures designed only for gravity loads: part III- Experimental Performance and Analytica study of a Structural Model. Technical report NCEER-92-0029.

Braga, F. and D'Anzi, P., 1994. Steel braces with energy absorbing devices: a design method to retrofit reinforced concrete existing buildings. *Italian-French symposium: Strengthening and repair of structures in seismic area,* Nice, France, 146-154.

Christopoulos, C. and Filiatrault, A., 2006. Principles of passive supplemental damping and seismic isolation. IUSS Press, Pavia, Italy.

Ciampoli, M. et al., 2003. Choice of an optimal Intensity Measure for the characterization of the damaging power of the ground motion. *Fourth International Conference of Earthquake Engineering and Seismology.*

Dall'Asta, A., Ragni, L., Tubaldi, E., Freddi, F., 2009. Design methods for existing r.c. frames equipped with elasto-plastic or viscoelastic dissipative braces, *XIII Convegno Nazionale ANIDIS: L'Ingegneria sismica in Italia*, Bologna, Italy.

El-Attar, A., R. N. White, et al., 1990. Shake table test of a 1/6 scale 2-story lightly reinforced concrete building. *Proceedings of the US National Conference on Earthquake Engineering*, 767-767.

El-Attar, A. G., R. N. White, et al., 1991. Shake table test of a 1/8 scale three-story reinforced concrete frame building designed primarily for gravity loads" *Proceedings of the Canadian Conference on Earthquake Engineering*, 639-639.

European Committee for Standardization (ECS), 2005. Eurocode 8 - Design of structures for earthquake resistance, EN1998, Brussels.

Güneyisi, E. M. and G. Altay, 2008. Seismic fragility assessment of effectiveness of viscous dampers in R/C buildings under scenario earthquakes. *Structural Safety* **30**(5), 461-480.

Hueste, M.D. and Bai, J.W., 2007. Seismic Retrofit of a Reinforced Concrete Flat-Slab Structure: Part II - Seismic Fragility Analysis. *Engineering Structures* **29**(6), 1178-1188.

Kasai, K., Fu, Y. and Watanabe, A., 1998. Passive control systems for seismic damage mitigation. *Journal of Structural Engineering* **124**(5), 501-512.

Katsanos, E.I., Sextos, A.G. and Manolis, G.D., 2009. Selection of earthquake ground motion records: A state-of-the-art review from a structural engineering perspective. *Soil Dynamics and Earthquake Engineering* **30**(4), 157-169.

Kwon, O.S. and Elnashai, A., 2006. The effect of material and ground motion uncertainty on the seismic
vulnerability curves of RC structure. *Engineering Structures* **28**(2), 289–303.

Liel, A.B., Haselton, C.B. and Deierlein, G.G., 2010. Seismic Collapse Safety of Reinforced Concrete Buildings: II. Comparative Assessment of Non-Ductile and Ductile Moment Frames, Journal of Structural Engineering (accepted for publication).

Mackie K. and Stojadinovic B. 2003. Seismic Demands for Performance-Based Design of Bridges. PEER Report 2003/16

Mazza, F. and Vulcano, A., 2008. Displacement-based design of dissipative braces at a given performance level of a framed building. 14th World Conference on Earthquake Engineering, Beijing, China.

McKenna, F., Fenves, G.L., Scott, M.H., 2006. OpenSees: Open system for earthquake engineering simulation. Pacific Earthquake Engineering Center, University of California, Berkeley, CA.

Panagiotakos, T.B., Fardis, M.N., 2001. Deformation of reinforced concrete members at yielding and ultimate. *ACI Structural Journal* **98**(2), 135-148.

Priestley, M. J. N., 1996. Displacement-based seismic assessment of existing reinforced concrete buildings. *Bulletin of the New Zealand National Society for Earthquake Engineering* **29**, 256-272.

Ponzo F.C., Di Cesare A., Arleo G., Totaro P., 2010. Protezione sismica di edifici esistenti con controventi dissipativi di tipo isteretico: aspetti progettuali ed esecutivi. *Progettazione sismica* **01**

Ramamoorthy, S., Gardoni, P. and Bracci, J., 2006. Seismic Fragility estimates for Reinforced Concrete Framed Buildings. Technical Report, Center for Design and Construction Integration, Texas A&M University.

Scott, M.H. and Fenves, G.L., 2006. Plastic hinge integration methods for force-based beam-column elements. *Journal of Structural Engineering* **132**(2), 244-252.

Soong, T.T. and Spencer, B.F., 2002. Supplemental energy dissipation: state-of-the-art and state-of-the-practice. *Engineering Structures* **24**(3), 243-259.

Vamvatsikos, D. and C. Allin Cornell, 2001. Incremental dynamic analysis. *Earthquake Engineering and Structural Dynamics* **31**, 491-514.